Theor Chem Account (2008) 119:421–427
DOI 10.1007/s00214-007-0397-0

REGULAR ARTICLE

Harmonic averaging of smooth permittivity functions in finite-difference Poisson–Boltzmann Electrostatics

Stephen T. Kottmann

Received: 11 September 2007 / Accepted: 29 October 2007 / Published online: 27 November 2007

Abstract Finite-difference Poisson–Boltzmann calculations offer an efficient and accurate means for electrostatic characterization of solvated molecules. However, discretization of charge and permittivity results in sensitive dependence on molecular position and orientation relative to the finite-difference grid. In this article, an improved method for limiting the error associated with discretization of the molecular volume, combining harmonic averaging between grid vertices and Gaussian-based smooth permittivity functions, is presented. While both these methods have the broader result of a smoothly varying permittivity, the Gaussian model represents a fundamental description of the dielectric boundary while harmonic averaging serves to provide information about the permittivity between grid points. Grid positional error is reduced by an order of magnitude in calculations of Born ion solvation energies, small molecule and protein solvation energies, and the solvation energy contribution to a protein-inhibitor complex.

Keywords Poisson–Boltzmann · Finite-difference · Grid-independence

1 Introduction

Implicit solvent models have become a valuable resource in the characterization of biochemical and macromolecule systems [1,2]. While explicit inclusion of solvent molecules is ostensibly the most accurate method, implicit solvent models have proven to reproduce the effects of the solvent environment in many systems while increasing computational efficiency [3–8]. Addition of explicit water molecules to a typical biomolecular system can increase the total number of atoms by an order of magnitude. Implicit solvent models replace the numerous solvent molecules with a continuum dielectric and seek to capture the average effects of the solution environment at the cost of detail in solute–solvent interactions.

The Poisson–Boltzmann equation (PBe) provides a robust and accurate method for calculating continuum electrostatic energies of molecules in solution environments and is often used as the standard to measure the viability of other implicit solvent models [9–11]:

$$\nabla\cdot(\epsilon(\mathbf{r})\nabla\phi(\mathbf{r})) - \bar{\kappa}^2(\mathbf{r})\sinh\left[\frac{e\phi(\mathbf{r})}{kT}\right] = -4\pi\rho(\mathbf{r}) \qquad (1)$$

where $\epsilon(\mathbf{r})$ is the permittivity defined by a low dielectric molecular cavity embedded in a high dielectric continuum, $\phi(\mathbf{r})$ is the electrostatic potential, $\rho(\mathbf{r})$ is the molecular charge distribution, e is the elementary charge, k the Boltzmann constant, T the absolute temperature, and $\bar{\kappa} = \kappa\sqrt{\epsilon}$ is a dielectric independent Debye–Huckel parameter. Equation 1 represents the "full", or non-linear, form of the Poisson–Boltzmann equation and is often linearized by the assumption that the potential, ϕ, is small in the ion accessible region.

In this model, the molecular system is discretized onto a set of vertices spanning the volume of the molecule and a surrounding solvent volume. The electrostatic potential can then be calculated by a variety of methods, including boundary-value finite-difference (FD) techniques [12,13]. Once the electrostatic potential is known, the electrostatic free energy of a set of discrete charges is obtained from,

$$G_{\text{elec}} = \frac{1}{2}\sum_i q_i\phi(\mathbf{r_i}) \qquad (2)$$

S. T. Kottmann (✉)
Department of Chemistry, Massachusetts Institute of Technology,
77 Massachusetts Ave., Cambridge, MA 02139, USA
e-mail: kottmast@mit.edu

for the linearized PBe, where q_i are the atomic charges located at positions $\mathbf{r_i}$. Traditionally, the solvation energy is obtained by computing the difference in electrostatic energy between a calculation with an inhomogeneous dielectric defined by a low dielectric molecular cavity embedded in a high dielectric medium, and a reference calculation with uniform dielectric [3]. However, it is also possible to calculate the solvation energy using a single calculation by first computing the induced polarization charges at the dielectric boundary followed by calculation of the Coulombic interaction between the solute charges and the polarization charges [14]. Although this method eliminates the necessity of a second PBe solution, the conventional reference calculation method is utilized in this work in order to maintain consistency as the definition of the dielectric boundary is changed.

Recently there has been a focus on incorporation of Poisson–Boltzmann electrostatics in molecular dynamics (MD) and Monte Carlo (MC) simulations [5,15–17]. These simulations derive particular benefit from the reduction in degrees of freedom offered by implicit solvent models. However, these applications require the repeated calculation of solvation energies (often millions of times) and represent a demanding implementation of the Poisson–Boltzmann equation. Such applications also call for the direct comparison of molecular solvation energies following translational, rotational, and conformational changes. However, one of the more challenging aspects of implementing the PBe model is stabilization of the energy calculation with respect to the molecular position and orientation on the FD grid [18–22]. The calculated electrostatic potential has significant dependence on the discretized maps of both the charge and dielectric, thus complicating such comparisons.

Charge discretization methods based on uniform charge distribution [18], antialiasing [19], and inverse quadratic interpolation [20] have been shown to significantly reduce the dependence of electrostatic calculations on the discretized map in comparison to the traditional point charge representation. Also, several methods have been proposed to smoothen the abrupt change in dielectric at the molecular surface in order to reduce positional error. This can be achieved by averaging of local dielectric values [19,21] or by the introduction of smoothly varying dielectric functions [20,22]. Naturally, molecular position and orientation error can also be decreased by reducing the grid spacing at the cost of greater computational demand. However, limiting this error to a level appropriate within the framework of a molecular mechanics simulation of even a moderately sized peptide can require grid dimensions beyond the range of acceptable computational efficiency.

In this article, a method combining Gaussian-based permittivity functions and harmonic averaging over FD grid lines is shown to reduce the positional error associated with the discretization of the molecular surface. A distinction should be made between a smooth dielectric model, such as the atom-centered Gaussian functions discussed below, and smoothing methods such as harmonic averaging. The smooth dielectric model addresses the physical reality of a discontinuity in the permittivity. However, harmonic averaging between grid vertices merely has the effect of smoothing the discretized dielectric boundary. By including more detailed information about the dielectric between two grid vertices, the position of the molecular surface is more precisely defined. Thus, we can combine the two methods, utilizing a physically reasonable smooth permittivity model while benefitting from increased knowledge of the permittivity between grid points. Ultimately, this results in the abilty to obtain acceptably small discretization error from larger grid scales. Computational costs of cubic grid-based methods typically scale proportionally to the cube of the grid size. Therefore the ability to utilize larger grid scales represents a significant and straightforward method to reduce computational time and memory demands, enabling larger and longer simulations of solvated biomolecules.

2 Methods

The grid constructed for finite-difference Poisson–Boltzmann calculations consists of a rectangular array of vertices, upon which the appropriate values for the charge, dielectric constant, and ionic strength must be assigned. These vertices effectively subdivide the space in and around the molecular volume into cubes centered around each vertex. Atomic charges are mapped by considering a constant charge density over the cube, while values for the dielectric are assigned to each face of the cube. These dielectric values are shared by neighboring cubes and mark the midpoints of grid lines connecting the grid vertices. Traditionally, points within the molecular interior are assigned a dielectric constant of ϵ_{solute} (typically 1–4) while points in the solvent region are assigned a value of $\epsilon_{\text{solvent}}$ ($\approx$78 for water), leading to a discontinuous step at the molecular surface.

As atoms move relative to the FD grid and vertices pass through the molecular surface, the abrupt change in dielectric causes significant fluctuations in the calculated electrostatic energies. Davis and McCammon [21] showed that the errors associated with the precipitous change in dielectric could be alleviated by harmonically averaging the permittivity over the grid line connecting two vertices, rather than solely taking the value at the midpoint. This conclusion was inspired by matching finite-difference theory to the analytical solution for a parallel plate capacitor. The result can also be obtained by the subdivision of a single grid line followed by application of one-dimensional finite-difference approximations and elimination of variables.

This averaging technique can be interpreted as an increase in the precision with which the location of the dielectric boundary is defined as more detailed information about the permittivity function has been included. The traditional, binary representation provides no further information than between which two grid points the molecular surface lies. By averaging along the grid line, we gain more precise information of where the boundary falls between the two grid points. This also produces the effect of a smoothly varying dielectric at the molecular surface, resulting in improved computational stability and convergence, although the fundamental model of the molecular surface is unchanged.

Alternatively, Grant et al. [20] proposed a smoothly varying dielectric function inspired by the physical necessity for continuously variable macroscopic properties and their previous success in describing molecular volumes by atomic Gaussians [23]. In this model, the dielectric is determined as

$$\epsilon(\mathbf{r}) = \epsilon_{\text{solute}} + (\epsilon_{\text{solvent}} - \epsilon_{\text{solute}})\, \mathrm{e}^{-A\rho_{\text{sum}}(\mathbf{r})} \tag{3}$$

$$\rho_{\text{sum}}(\mathbf{r}) = \sum_i p_A \mathrm{e}^{-\kappa r_i^2/\sigma_i^2} \tag{4}$$

where the sum is carried out over the atoms of the molecule, r_i and σ_i are the distance from and radius of atom i, respectively, and p_A, κ, and A are dimensionless adjustable parameters. The Gaussian model imparts several benefits. Besides offering an arguably more physically realistic basis, the atomic Gaussian molecular volume provides a simpler construction than the molecular surface. Differentiability with respect to atomic position allows for the direct calculation of solvent forces and subsequent incorporation into molecular dynamics simulations. Also, similar to the averaging technique, this smoothly varying permittivity function provides computational stability and improved convergence.

Although both these methods have the broader result of a smoothly varying permittivity, it is important to mark the distinction between the atom-centered Gaussian function as a fundamental model of the solute–solvent boundary and harmonic averaging as a technique to obtain more detailed information of the discretized molecular surface at a given grid scale. Here we seek to combine the benefits of each method by applying the harmonic averaging technique of Davis and McCammon to the atom-centered Gaussian-based permittivity functions. To this end, the Gaussian volume function is first evaluated at adjacent grid points i and $i+1$ by Eq. 4 to give ρ_i and ρ_{i+1}, respectively. With a continuous definition of the permittivity, the harmonic average is replaced by the analagous integral equation, written as

$$\begin{aligned}\epsilon(\mathbf{r}) &= \frac{(\rho_{i+1} - \rho_i)}{\int_{\rho_i}^{\rho_{i+1}} d\rho[\epsilon_{\text{solute}} + (\epsilon_{\text{solvent}} - \epsilon_{\text{solute}})\exp(-A\rho)]^{-1}} \\ &= \frac{\epsilon_{\text{solute}}(\rho_{i+1} - \rho_i)}{(\rho_{i+1} - \rho_i) - A^{-1}\ln(\epsilon_{i+1}/\epsilon_i)}\end{aligned} \tag{5}$$

where ϵ_i and ϵ_{i+1} are the dielectric evaluated by Eq. 3 at the grid vertices. This method retains the benefits of the physically appealing smooth permittivity function, while also capitalizing on the the increased positional stability of the harmonic averaging technique.

In all calculations, solvation energies were calculated with solute and solvent dielectric constants of 1 and 80, respectively. Charges were mapped to the FD grid following the inverse quadratic interpolation proposed by Grant et al. [20]. The finite-difference Poissson–Boltzmann equation was solved numerically by red-black Gauss–Seidel iterations, with convergence assumed when the calculated electrostatic energy changed by less than 1×10^{-6} kcal/mol. Solvation energies were calculated by taking the difference from a uniform dielectric reference calculation. Ionic strength was set to zero in all calculations, and boundary values were set according to the Coulombic potential.

3 Results and discussion

Born ion, small molecule, and protein solvation energy calculations are often used to demonstrate the efficacy of implicit solvent models at various system sizes [18–21]. The Born ion provides a simple, clear testing ground as the solvation energy of a single ion with charge q and radius σ is available analytically for comparison as

$$G_{\text{Born}} = \frac{q^2}{8\pi\epsilon_0\sigma}\left(\frac{1}{\epsilon_{\text{solvent}}} - \frac{1}{\epsilon_{\text{solute}}}\right) \tag{6}$$

In order to illustrate practical application of this method, solvation energy calculations were also performed on a set of small molecules and proteins from the Protein Data Bank (http://www.rcsb.org/pdb). Finally, the solvation contribution to the binding energy of the thrombin–NAPAP complex is used to demonstrate application to computational binding simulations. In order to assess positional error, the solvation energy of each ion or small molecule was calculated at 100 random positions relative to the FD grid. Protein solvation energies were calculated at 20 random positions relative to the FD grid. The standard deviation and range, defined as the difference between the maximum and minimum values, of calculated solvation energies were used to evaluate the positional stability of four dielectric models: the traditional discontinuous molecular surface (MS), the harmonically averaged molecular surface (MS-HA), the Gaussian-based permittivity (GAUSS), and our harmonically averaged-Gaussian-based permittivity method (GAUSS-HA).

The solvation energy of a single ion with radius $\sigma = 2$ Å and unit charge $q = 1$ was evaluated at 100 grid positions for grid spacings in the range of 0.1–1.0 Å. Figure 1a illustrates the average error in the Born ion solvation energy calculation

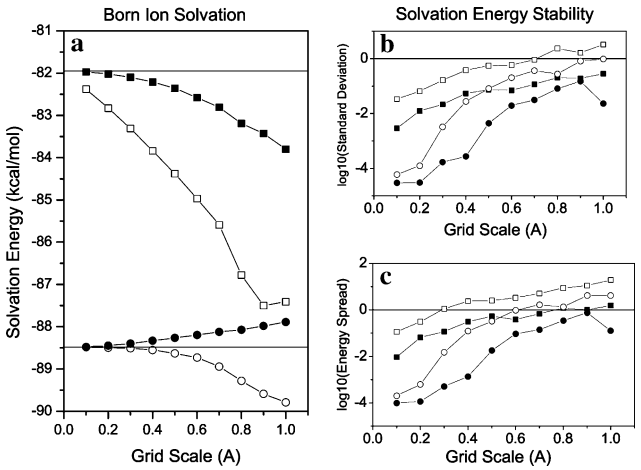

Fig. 1 Calculation of Born ion solvation energies as a function of grid spacing for each of the four dielectric models: (*open square*) Traditional molecular surface, (*filled square*) Harmonically averaged molecular surface, (*open circle*) Gaussian atomic volume function, and (*closed circle*) Harmonically averaged Gaussian atomic volume function. **a** Ion solvation energy. Each point represents the average solvation energy calculated at 100 random positions relative to the finite-difference grid. The horizontal line at −81.95 kcal/mol represents the theoretical solvation energy of a 2 Å Born ion in water (ϵ_{solv}=78), while the horizontal line at −88.47 kcal/mol represents the fine grid solvation energy for the Gaussian model and serves as a guide to the eye. **b** Standard deviation of the calculated solvation energies. **c** Energy spread is the difference between the maximum and minimum calculated solvation energies. Note that **b** and **c** are on a logarithmic scale

over the range of grid scales. Solvation energies are known to be highly sensitive to the description of the molecular surface and therefore force-fields are often re-parameterized for optimum accuracy [10,24,25]. This is not a surprising result considering that solvation energy in the continuum representation is equated with the build-up of induced polarization charge at the dielectric interface. Smooth permittivity models represent the region of induced polarization charge as a three-dimensional volume, whereas in the discrete molecular surface model polarization charges exist only on a two-dimensional surface. This difference in the definition of the dielectric boundary and position of induced charges will considerably alter the solvation energy. It is apparent that this is the case with the Gaussian-based models, as both converge at fine grid scale to a solvation energy of $G_{solv} = -88.47$ kcal/mol rather than the analytical value of $G_{Born} = -81.95$ kcal/mol. Optimal re-parameterization of atomic radii is also specific to the charge parameters of the force-field in use and must be considered for each application. In the current work we do not consider such a re-parameterization, but refer the reader to Swanson et al. [24,25], who have demonstrated both the rescaling of current force-field parameters as well as successful optimization of new parameter sets for smooth permittivity functions. In the absence of this re-parameterization, focus should instead be placed on the error relative to the fine grid value for the Gaussian-based models. The increased accuracy achieved through harmonic averaging is very apparent in the MS models, and can also be seen in the Gaussian-based models at larger grid scales. The stabilizing benefits of harmonic averaging are illustrated in Fig 1b, c by examining the standard deviation and range of solvation energies, respectively, for the 100 repeated calculations at each grid scale. For a desired stability characterized by a standard deviation of 10^{-2} kcal/mol, the MS-HA model requires a grid scale of 0.2 Å, the GAUSS model requires a grid scale of slightly less than 0.4 Å, while the GAUSS-HA model achieves this level of stability at a grid scale of 0.6 Å, with an absolute error of less than 0.3 kcal/mol.

The second test of combining Gaussian-based permittivity functions and harmonic averaging was the calculation of molecular solvation energies. A set of eight small molecules and four proteins were used to test the accuracy and stability of the three reference dielectric models and our new combined method. Atom charge and radius parameters were taken from the optimized parameters for liquid simulations [27] (OPLS), with the exception of charged hydrogens whose radius was set as 0.8 Å rather than 0.0, as such a radius is inappropriate for a molecular volume-based solvation energy calculation. Interior and exterior dielectric constants were set to 1 and 80, respectively, as consistent with the OPLS force field. Table 1 shows the solvation energy, standard deviation, and range of energies for each molecule calculated at a relatively large grid spacing of 1 Å. Solvation energies are similar between all methods, although it is again apparent, particularly for the protein energies, that the Gaussian models should be re-parameterized for optimal agreement with the molecular surface models.

Perhaps the most straightforward approach to accelerating Poisson–Boltzmann calculations is the increase of grid scale. We have chosen here a large grid scale to emphasize the stability imparted by the combination of a smooth dielectric model and the averaging technique. Accurate work normally requires a grid scale of 0.5 Å or less. Even at a large grid scale, the GAUSS-HA model produces standard deviations in small molecule solvation energies of less than 0.35 kcal/mol. Also, the range of calculated energies, defined as the difference between the maximum and minimum values, for each of the small molecules is comparable to the thermal energy, k_BT; an important comparison when considering Monte Carlo simulations, for example. Protein calculations are similarly stabilized, exemplified by the relative standard deviation of a ferrodoxin protein (PDB# 2FDN) solvation energy, which is limited to 0.03%.

For application of the GAUSS-HA model to molecular dynamics simulations, it must be verified that solvation forces are also stabilized with respect to molecular position on the finite-difference grid at large grid scales. Figure 2 illustrates the accuracy and stability of atomic solvation forces for each

Table 1 Grid stability in solvation energy calculations (Solvation energies for each small molecule were calculated at 100 random positions relative to the finite-difference grid, while each protein was sampled at 20 random positions. All energies are reported in kcal/mol and given as the mean ± the standard deviation. Atomic parameters were taken from the optimized parameters for liquid simulations (OPLS) [27], except for charged hydrogens which have a radius of zero in the OPLS force field. Such a radius is inappropriate for Poisson electrostatic calculations, and therefore has been reset to 0.8 Å. A grid spacing of 1.0 Å and relative dielectric constants of 1 and 80 were used for the interior and exterior values, respectively, for all calculations. The range is the difference between the maximum and minimum calculated solvation energies. $C7^{eq}$-Ala, C5-Ala, and α_R-Ala represent different conformations of the alanine dipeptide, as described elsewhere [28]

	MS		MS-HA		Gauss		Gauss-HA	
Molecule	E_{solv}	Range	E_{solv}	Range	E_{solv}	Range	E_{solv}	Range
Methanol	-10.26 ± 1.52	8.49	-8.70 ± 0.55	1.94	-8.47 ± 0.60	2.24	-7.15 ± 0.17	0.66
Ethanol	-9.86 ± 1.46	5.79	-8.37 ± 0.30	1.43	-7.89 ± 0.48	1.75	-6.49 ± 0.12	0.59
2-Propanol	-9.80 ± 1.63	5.96	-8.25 ± 0.29	1.48	-7.78 ± 0.62	2.68	-6.32 ± 0.15	0.65
Acetone	-6.08 ± 0.90	4.16	-5.29 ± 0.11	0.55	-4.94 ± 0.37	1.64	-4.33 ± 0.06	0.23
Methyl acetate	-5.41 ± 0.79	3.44	-4.52 ± 0.18	0.78	-4.18 ± 0.29	1.35	-3.53 ± 0.12	0.43
Acetic acid	-96.75 ± 6.57	23.91	-90.77 ± 0.66	3.26	-90.54 ± 3.05	12.24	-85.09 ± 0.34	1.31
Acetamide	-15.25 ± 1.18	5.59	-13.02 ± 0.32	1.51	-12.96 ± 0.53	2.41	-10.86 ± 0.17	0.64
$C7^{eq}$-Ala	-20.84 ± 1.84	7.82	-17.82 ± 0.39	1.87	-16.83 ± 0.71	3.11	-14.07 ± 0.16	0.67
C5-Ala	-23.74 ± 1.93	7.24	-20.72 ± 0.31	1.15	-19.44 ± 0.84	3.54	-16.95 ± 0.22	0.81
α_R-Ala	-24.50 ± 1.57	6.21	-21.76 ± 0.37	1.95	-20.62 ± 0.70	2.93	-18.22 ± 0.13	0.48
1GQV	-3587.89 ± 23.89	98.97	-3273.01 ± 9.27	48.92	-2837.55 ± 6.59	27.71	-2550.87 ± 1.60	6.33
1HJE	-160.34 ± 4.95	22.69	-140.02 ± 1.91	8.85	-119.00 ± 1.96	9.02	-103.01 ± 0.41	1.81
1KCH	-651.35 ± 9.71	46.10	-567.69 ± 4.47	19.92	-432.16 ± 1.74	7.91	-364.98 ± 0.59	2.43
2FDN	-6641.30 ± 24.39	99.88	-6497.97 ± 4.93	23.10	-6367.31 ± 8.78	36.00	-6238.17 ± 1.84	7.25

model, comparing the forces calculated at a grid scale of 1.0 Å to those calculated at a grid scale of 0.1 Å. Forces were calculated at 25 random molecular positions relative to the finite difference grid for a subset of atoms from the test structures listed in Table 1. Forces in the harmonically averaged models show improved accuracy, while the harmonically averaged Gaussian model demonstrates significantly improved stability in the standard deviation of the calculated forces. The coarse grid relative standard deviation is reduced on average by a factor of two by application of harmonic averaging, from 146.01% for MS to 75.25% for MS-HA, and from 24.49% for GAUSS to 11.60% for GAUSS-HA.

Finally, the GAUSS-HA model is demonstrated in comparison to the other three models in calculating the solvation contribution to the binding energy of the bovine thrombin-NAPAP (N^{α}-(2-naphthyl-sulphonyl-glycyl)-D-*p*-amidino-phenylalanyl-piperidine) complex [26]. The input structures were prepared from the Protein Data Bank file (1ets) by removing waters and ensuring neutrality of the thrombin protein. This coagulation protein–inhibitor complex consists of 2,652 atoms, and was chosen as representative of general protein–ligand binding experiments. Atom and radius parameters were again taken from the OPLS force field, with interior and exterior dielctric constants of 1 and 80. Solvation energy calculations were carried out at 20 random positions relative to the finite difference grid. The contribution to binding energy was calculated as the difference in mean solvation energies between the complex and its component parts, and standard deviations were combined to yield the standard deviation of the binding energy. Figure 3 shows the difference in solvation energies over a range of grid spacings from 0.3 to 1.4 Å for each dielectric model. Once again, it is evident that the absolute energy calculated with the Gaussian model differs from the molecular surface model when using the same atomic parameters, and comparison should be made to the energies calculated at fine grid spacing. The GAUSS model alone offers similar accuracy and stability at large grid scales to the MS-HA model. Application of the averaging technique to the Gaussian-based permittivity functions further stabilizes the calculation, reducing the standard deviation of calculated binding energies by a factor of 3–5 and absolute errors by a factor of 2–3 over the range of grid scales.

Harmonic averaging in the MS-HA model adds a significant computational cost to the grid initialization routine. For the thrombin–NAPAP complex on a 1.0 Å grid, the initialization CPU time for the MS model was 2.1 s on a single 2.4-GHz Intel Xeon processor. Ten point subdivision of molecular surface-spanning grid lines and harmonic averaging increased the initialization time to 14 s. However, in the case of the Gaussian model, there was no increase in initialization time. Initialization for the GAUSS model involves evaluation

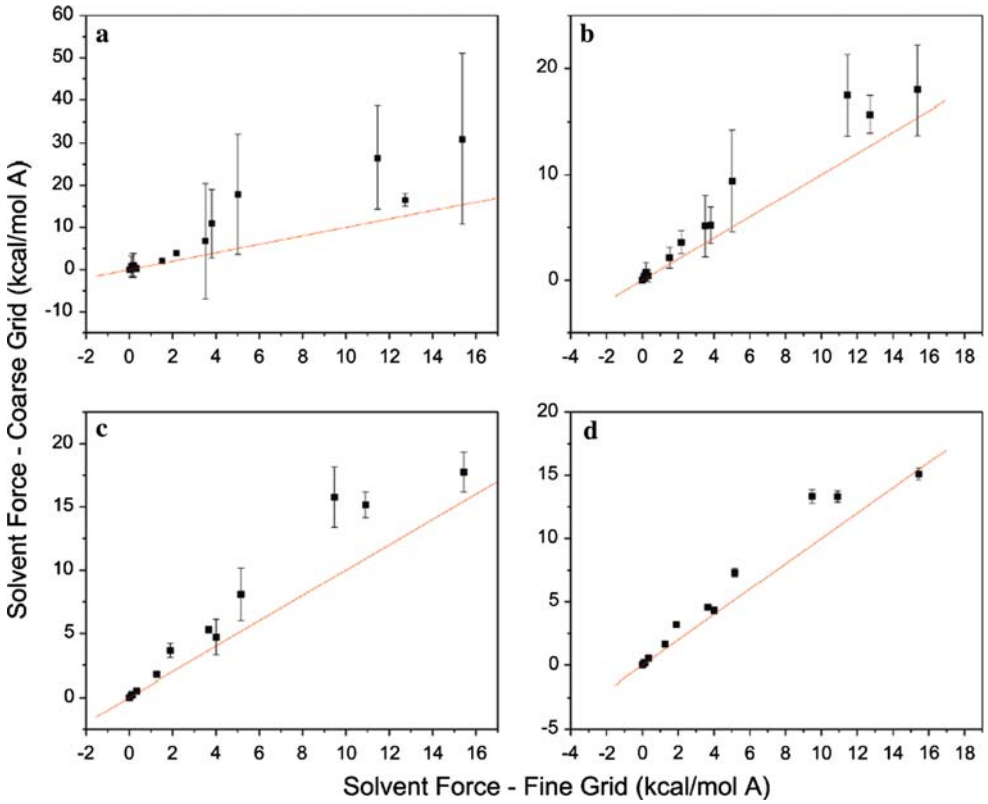

Fig. 2 Solvation forces for a subset of atoms from the test structures listed in Table 1 comparing coarse grid scale calculations (1.0 Å) to forces calculated at a fine grid scale (0.1 Å). Data points represent the average force for each atom calculated at 25 random molecular positions relative to the finite-difference grid, with standard deviations represented by error bars, and the line ($y = x$) as a guide for the eye. **a** MS model, **b** MS-HA model, **c** GAUSS model, and **d** GAUSS-HA model

of the Gaussian volume and dielectric, Eqs. 3 and 4, at the midpoint of each grid line. However, Eq. 5 includes the Gaussian volume and dielectric at the grid vertices only, and explicit subdivision of grid lines is not necessary. Therefore, the minimal computational cost of evaluating the harmonic average by Eq. 5 is recovered by evaluating the Gaussian density and dielectric at the grid vertices only, rather than at the midpoints of each grid line. Initialization times were 2.2 and 2.1 s for the GAUSS and our GAUSS-HA models, respectively. It has been demonstrated by Fogolari et al. [16], among others that solvation forces need not be updated at each time step in molecular dynamics applications. Following arguments based on the orientational dielectric relaxation time of water (≈10 ps) and the average lifetime of a hydrogen bond in bulk water (≈4 ps), a molecular dynamics protocol was developed in which Poisson–Boltzmann solvation forces were updated at an interval of 1 ps and combined by weighted average with previous PB forces in order to smooth fluctuations. Native protein structures were preserved over a 1 ns trajectory through this periodically updating scheme. Because it is not necessary to evaluate solvation forces at each time step, PB computation times on the order of a few seconds should not be seen as prohibitive in the application to MD simulations.

4 Conclusions

The Poisson–Boltzmann model provides an efficient alternative to explicit inclusion of solvent in simulations of biomolecules. However, calculated solvation energies have high sensitivity to the discretization of charge and permittivity functions in finite-difference calculations. For applications such as molecular mechanics simulations, where direct comparison of energies following translational, rotational, and conformational changes are required, this sensitivity necessitates fine grid scales for accurate, stable, and grid independent energy calculations. This work shows that application of harmonic averaging to Gaussian-based permittivity functions significantly reduces the positional error associated with the discretization of the molecular surface, allowing the range of acceptable accuracy and stability to be extended to larger grid-scales. This represents a straightforward and significant increase in computational efficiency, as computational

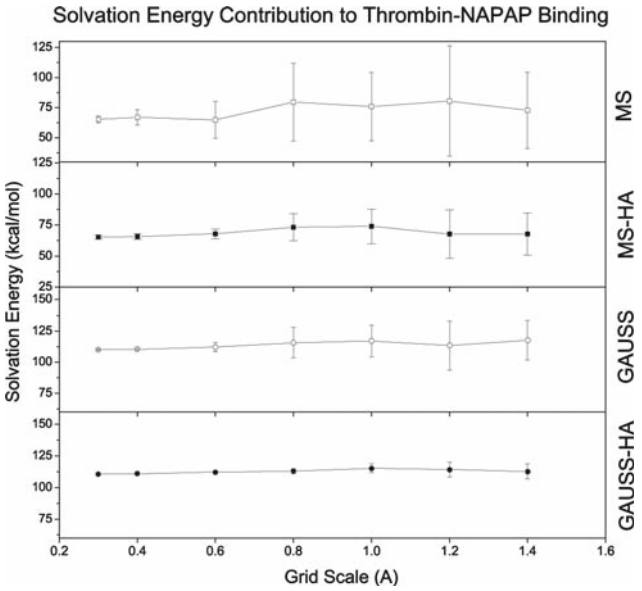

Fig. 3 Solvation energy contribution to bovine thrombin–NAPAP [26] binding energy. Each point represents the difference in solvation energy between the complex and its individual components, each averaged over 20 random positions relative to the finite-difference grid. Error bars represent the standard deviation. From *top* to *bottom*, *MS* the traditional molecular surface model, *MS-HA* harmonically averaged molecular surface, *GAUSS* Atomic Gaussian volume descriptors, *GAUSS-HA* harmonically averaged atomic Gaussian volume descriptors

resources for cubic grid-based methods typically scale proportionally to the cube of the grid size.

Acknowledgements We thank Angela M. Belcher, Peter J. Rossky, and Ahmad S. Khalil for helpful discussions. Financial support was provided by the Army Research Office Institute of Collaborative Biotechnologies.

References

1. Honig B, Nicholls A (1995) Science 268:1144–1149
2. Gilson MK (1995) Curr Opin Struct Biol 5:216–223
3. Sitkoff D, Sharp KA, Honig B (1994) J Phys Chem 98:1978–1988
4. Sitkoff D, Ben-Tal N, Honig B (1996) J Phys Chem 100:2744–2752
5. Prabhu NV, Zhu P, Sharp KA (2004) J Comput Chem 25:2049–2064
6. Wagoner J, Baker NA (2004) J Comput Chem 25:1623–1629
7. Zacharias M, Luty BA, Davis ME, McCammon JA (1994) J Mol Biol 238:455–465
8. Misra VK, Sharp KA, Friedman RA, Honig B (1994) J Mol Biol 238:245–263
9. David L, Luo R, Gilson MK (2000) J Comput Chem 21:295–309
10. Feig M, Onufriev A, Lee MS, Im W, Case DA, Brooks CLIII (2004) J Comput Chem 25:265–284
11. Gohlke H, Case DA (2004) J Comput Chem 25:238–250
12. Davis ME, McCammon JA (1989) J Comput Chem 10:386–391
13. Nicholls A, Honig B (1991) J Comput Chem 12:435–445
14. Rocchia W, Sridharan S, Nicholls A, Alexov E, Chiabrera A, Honig B (2002) J Comput Chem 23:128–137
15. Luo R, David L, Gilson MK (2002) J Comput Chem 23:1244–1253
16. Fogolari F, Brigo A, Molinari H (2003) Biophys J 85:159–166
17. Kollman PA, Massova I, Reyes C, Kuhn B, Huo S, Chong L, Lee M, Lee T, Duan Y, Wang W et al (2000) Acc Chem Res 33:889–897
18. Bruccoleri RE (1993) J Comput Chem 14:1417–1422
19. Bruccoleri RE, Novotny JR, Davis ME, Sharp KA (1997) J Comput Chem 18:268–276
20. Grant JA, Pickup BT, Nicholls A (2001) J Comput Chem 22:608–640
21. Davis ME, McCammon JA (1991) J Comput Chem 12:909–912
22. Im W, Beglov D, Roux B (1998) Comput Phys Commun 111:59–75
23. Grant JA, Pickup BT (1995) J Phys Chem 99:3503–3510
24. Swanson JMJ, Adcock SA, McCammon JA (2005) J Chem Theory Comput 1:484–493
25. Swanson JMJ, Wagoner JA, Baker NA, McCammon JA (2007) J Chem Theory Comput 3:170–183
26. Brandstetter H, Turk D, Hoeffken HW, Grosse D, Sturzebecher J, Martin PD, Edwards BFP, Bode W (1992) J Mol Biol 226:1085–1099
27. Jorgensen WL, Tirado-Rives J (1988) J Am Chem Soc 110:1657–1666
28. Brooks CL III, Case DA (1993) Chem Rev 93:2487–2502